

Time-dependent Monte Carlo simulations of the critical and Lifshitz points of the ANNNI model.

Roberto da Silva*

*Instituto de Física, Universidade Federal do Rio Grande do Sul, Av. Bento Gonçalves,
9500 - CEP 91501-970, Porto Alegre, Rio Grande do Sul, Brazil*

Nelson Alves Jr.[†] and Jose Roberto Drugowich de Felicio[‡]

*Faculdade de Filosofia, Ciências e Letras de Ribeirão Preto,
Universidade de São Paulo, Avenida Bandeirantes,
3900 - CEP 14040-901, Ribeirão Preto, São Paulo, Brazil*

In this work, we study the critical behavior of second order points and specifically of the Lifshitz point (LP) of a three-dimensional Ising model with axial competing interactions (ANNNI model), using time-dependent Monte Carlo simulations. First of all, we used a recently developed technique that helps us localize the critical temperature corresponding to the best power law for magnetization decay over time: $\langle M \rangle_{m_0=1} \sim t^{-\beta/\nu z}$ which is expected of simulations starting from initially ordered states. Secondly, we obtain original results for the dynamic critical exponent z , evaluated from the behavior of the ratio $F_2(t) = \langle M^2 \rangle_{m_0=0} / \langle M \rangle_{m_0=1}^2 \sim t^{3/z}$, along the critical line up to the LP. Finally, we explore all the critical exponents of the LP in detail, including the dynamic critical exponent θ that characterizes the initial slip of magnetization and the global persistence exponent θ_g associated to the probability $P(t)$ that magnetization keeps its signal up to time t . Our estimates for the dynamic critical exponents at the Lifshitz point are $z = 2.34(2)$ and $\theta_g = 0.336(4)$, values very different from the 3D Ising model (ANNNI model without the next-nearest-neighbor interactions at z -axis, i.e., $J_2 = 0$) $z \approx 2.07$ and $\theta_g \approx 0.38$. We also present estimates for the static critical exponents β and ν , obtained from extended time-dependent scaling relations. Our results for static exponents are in good agreement with previous works

I. INTRODUCTION

A. Modulated systems and the Lifshitz point

In condensed matter physics there are several models presenting spatial modulated structures of some local property, such as, for instance, the position of the particles, the magnetization and the charge density [1]. Such modulation can be commensurate or incommensurate in relation to the underlying lattice. A phase is named commensurate if the ratio between the period of the modulation and the period of the lattice is a rational number. Otherwise, the phase is named incommensurate. The basic mechanism leading to modulation is the competition between interactions favoring distinct orderings [2]. For example, the modulated structures observed in rare-earth metals [3] were interpreted as a consequence of the competition generated by the spatially oscillatory interaction RKKY [4–6]. In order to explain the spatial modulation found in Erbium, Elliott introduced an Ising model [7], twenty years later named ANNNI (Axial-Next-Nearest-Neighbor Ising) model [8]. It is one of the simplest models able to exhibit a rich phase diagram containing a complex region of spatially modulated phases [9–11]. The model is defined by the Hamiltonian

$$\mathcal{H} = - \sum_{x, y, z} [J_0(\sigma_{x+1, y, z} + \sigma_{x, y+1, z}) + J_1 \sigma_{x, y, z+1} + J_2 \sigma_{x, y, z+2}] \sigma_{x, y, z}$$

where $\sigma_{x, y, z} = \pm 1$ is an Ising spin variable at the site (x, y, z) of a simple cubic lattice, J_0 is the nearest neighbor interaction in the xy planes, J_1 and J_2 are the nearest and next-nearest-neighbor interactions in the z direction. Here J_1 and J_2 compete and may have opposite or same signs. However, when J_1 and J_2 have opposite signs, the competition between them may give rise to the modulated phases.

The mean-field phase diagram of the model displaying the main commensurate phases in the plane of the reduced temperature kT/J_1 against the competition parameter $-J_2/J_1$, shown in Fig. 1, was obtained in the beginning of the eighties [12] and is divided in three major regions: the modulated region (M), the paramagnetic (P) and the ferromagnetic (F) phases. In this diagram, as well as in the whole paper, we make $J_0 = J_1$. The paramagnetic phase is separated from the ferromagnetic phase and from the modulated region by critical lines P-F and P-M respectively. On the other hand, a first-order transition (F-M) takes place between the ferromagnetic and the modulated region. The critical line P-M belongs to the universality class of the XY model, whereas the critical line P-F presents Ising-like critical behavior [13]. The transition lines P-F, P-M and F-M meet at the Lifshitz point (LP), introduced theoretically by Hornreich et al. [14]. The location of the LP in the phase diagram of the

* rdasilva@if.ufgrs.br

† nalves@if.usp.br

‡ drugo@usp.br

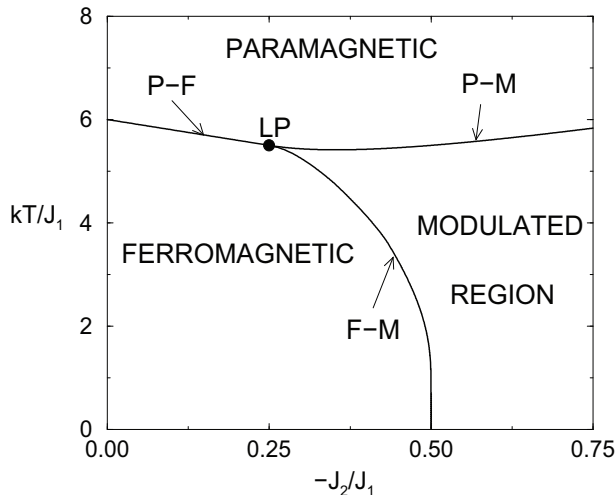


FIG. 1. Mean Field phase diagram of the ANNNI Model, displaying the ferromagnetic phase, the paramagnetic phase and the modulated region. The critical lines P-F and P-M meet the first order phase transition line F-M at the Lifshitz point (LP) (see text).

ANNNI model was obtained for the first time from high temperature series technique [15]. However, the precise location of the LP is difficult to obtain because, close to it, one meets the challenging task of dealing with modulated phases of very large periods. Thus, latter attempts to locate the LP were made. Single spin-flip Monte Carlo simulations were performed along the P-F critical line towards the LP [16, 17], thus avoiding the modulated region. Despite the successful results obtained from these works, it was only recently that the Lifshitz point was located with high precision [18] by means of a new variation of the cluster Wolf algorithm [19]. Concerning the critical properties of the LP, it was shown that this multicritical point belongs neither to the universality class of the XY model nor to the one of Ising model [14]. This fact gave rise to much interest in the study of the particular critical behavior of a LP. Thus, the critical properties of the LP found in the phase diagram of the ANNNI model were widely studied by several approaches [20, 21], among them ϵ -expansions [14], high temperature series technique [21] and Monte Carlo simulations [17]. Experimentally, the most complete results concerning the LP were obtained for the magnetic compound MnP, which exhibits a LP belonging to the universality class of the LP present in the ANNNI model [22–24]. Here it is important to mention that although this model has been widely explored by methods from equilibrium statistical mechanics, there are no results for the 3D ANNNI model obtained by an approach that deals with MC simulations performed far from equilibrium [25] that will be employed in this paper. However we remark that several works in the literature have used previously a dynamical approach to study the Lifshitz points. For example

the critical dynamics of relaxation of the model near the Lifshitz point has been studied by the ϵ -expansion and the exponent z was numerically estimated for uniaxial and biaxial cases [26]. Alternatively, in [27] the growth of a order parameter is studied when a system at Lifshitz point is quenched from the homogeneous disordered state to the ordered state where correlation and structure factors after quench in this system are analyzed via Renormalization Group method. Numerical estimates of exponent z are supplied in this same reference. Studies about dynamics of ANNNI model were developed but in two dimensional versions of the model but such works do not explore critical properties. For example, in [28], [29], the kinetics of domain growth of the one and two-dimensional anisotropic ANNNI model was explored via Monte Carlo methods using Glauber and Heat-Bath multispin dynamics respectively.

In the next subsection we briefly present the non-equilibrium approach to be used in our analysis.

B. Non-equilibrium Critical dynamics

The study of critical properties originated from statistical fluctuations of spin systems became possible in non-equilibrium stage after the seminal ideas of Janssen, Schaub and Schmittmann [30] and Huse [31]. By quenching systems from high temperatures to the critical one, they have shown that universality and scaling behavior appear even in the early stages of time evolving, via renormalization group techniques and numerical calculations respectively. Hence, by using short time dynamics, one can often circumvent the well-known problem of the critical slowing down that plagues investigations of the long-time regime.

Here, we briefly review finite size scaling in the dynamics relaxation of spin systems. We present our alternative derivation of some power laws in the short time dynamics context. Readers, who want a more complete review about this topic, may want to read [32, 33].

This topic is based on time dependent simulations, and it constitutes an important issue in the context of phase transitions and critical phenomena. Such methods can be applied not only to estimate the critical parameters in spin systems, but also to calculate the critical exponents (static and dynamic ones) through different scaling relations by setting different initial conditions.

The dynamic scaling relation obtained by Janssen *et al.* for the k -th moment of the magnetization, is written as

$$\langle M^k \rangle(t, \tau, L, m_0) = b^{-k\beta/\nu} \langle M^k \rangle(b^{-z}t, b^{1/\nu}\tau, b^{-1}L, b^{x_0}m_0), \quad (1)$$

where the arguments are: the time t ; the reduced temperature $\tau = (T - T_c)/T_c$, with T_c being the critical one, the lattice linear size L and initial magnetization m_0 . Here, the operator $\langle \dots \rangle$ denotes averages over different configurations due to different possible time evolutions

from each initial configuration compatible with a given m_0 .

On the right-hand side of the equation, one has: an arbitrary spatial rescaling factor b ; an anomalous dimension x_0 related to m_0 . The exponents β and ν are the equilibrium critical exponents associated with the order parameter and the correlation length, respectively. The exponent z is the dynamic one, which characterizes the time correlations in equilibrium. After choosing $b^{-1}L = 1$, $T = T_c(\tau = 0)$, and $k = 1$ we obtain $\langle M \rangle(t, L, m_0) = L^{-\beta/\nu} \langle M \rangle(L^{-z}t, L^{x_0}m_0)$.

Denoting $u = tL^{-z}$ and $w = L^{x_0}m_0$, one has: $\langle M \rangle(u, w) = \langle M \rangle(L^{-z}t, L^{x_0}m_0)$. The derivative with respect to L is:

$$\frac{\partial \langle M \rangle}{\partial L} = (-\beta/\nu)L^{-\beta/\nu-1} \langle M \rangle(u, w) + L^{-\beta/\nu} \left[\frac{\partial \langle M \rangle}{\partial u} \frac{\partial u}{\partial L} + \frac{\partial \langle M \rangle}{\partial w} \frac{\partial w}{\partial L} \right],$$

where we have explicitly: $\partial u / \partial L = -ztL^{-z-1}$ and $\partial w / \partial L = x_0 m_0 L^{x_0-1}$. In the limit $L \rightarrow \infty$, $\partial_L \langle M \rangle \rightarrow 0$, one has: $x_0 w \frac{\partial \langle M \rangle}{\partial w} - zu \frac{\partial \langle M \rangle}{\partial u} - \beta/\nu \langle M \rangle = 0$. The separability of the variables u and w in $\langle M \rangle(u, w) = M_1(u)M_2(w)$ leads to $x_0 w M_2' / M_2 = \beta/\nu + zu M_1' / M_2$, where the prime means the derivative with respect to the argument. Since the left-hand-side of this equation depends only on w and the right-hand-side depends only on u , they must be equal to a constant c . Thus, $M_1(u) = u^{(c/z)-\beta/(\nu z)}$ and $M_2(w) = w^{c/x_0}$, resulting in $\langle M \rangle(u, w) = m_0^{c/x_0} L^{\beta/\nu} t^{(c-\beta/\nu)/z}$. Returning to the original variables, one has: $\langle M \rangle(t, L, m_0) = m_0^{c/x_0} t^{(c-\beta/\nu)/z}$.

On one hand, choosing $c = x_0$ and calculating $\theta = (x_0 - \beta/\nu)/z$, at criticality ($\tau = 0$), we obtain

$$\langle M \rangle_{m_0} \sim m_0 t^\theta \quad (2)$$

corresponding to a regime under small initial magnetization. This can be observed by a finite time scaling $b = t^{1/z}$ in equation (1), at critical temperature ($\tau = 0$) which leads to $\langle M \rangle(t, m_0) = t^{-\beta/(\nu z)} \langle M \rangle(1, t^{x_0/z} m_0)$. Defining $x = t^{x_0/z} m_0$, an expansion of the averaged magnetization around $x = 0$ results in: $\langle M \rangle(1, x) = \langle M \rangle(1, 0) + \partial_x \langle M \rangle|_{x=0} x + \mathcal{O}(x^2)$. By construction $\langle M \rangle(1, 0) = 0$, since $x = t^{x_0/z} m_0 \ll 1$ and $\partial_x \langle M \rangle|_{x=0}$ is a constant, discarding the quadratic terms we obtain the expected power law behavior $\langle M \rangle_{m_0} \sim m_0 t^\theta$. This anomalous behavior of initial magnetization is valid only for a characteristic time scale $t_{\max} \sim m_0^{-z/x_0}$.

On the other hand, the choice $c = 0$ corresponds to the case which the system does not depend on the initial trace and $m_0 = 1$ leads to simple power law:

$$\langle M \rangle_{m_0=1} \sim t^{-\beta/(\nu z)} \quad (3)$$

that similarly corresponds to decay of magnetization for $t > t_{\max}$. The evaluation of critical exponents θ and

$\beta/(\nu z)$ via Monte Carlo simulations concerns taking averages over different runs. In the second case, simpler simulations are considered because since the system starts from the ferromagnetic (ordered) initial state. However, the first one is somewhat difficult to deal with, once it demands working with prepared initial states with a precise value of m_0 (sharp preparation), besides the delicate limit $m_0 \rightarrow 0$.

An alternative way to determine this exponent was proposed by Tomé and Oliveira [34], where it was shown that the time correlation function of the order parameter also follows a power law scale form at the short-time regime, i. e.

$$Q(t) = \langle M(0)M(t) \rangle \sim t^\theta. \quad (4)$$

The main advantage in the use of Eq. (4) is that one does not need to fix precisely the initial order parameter m_0 . The only requirement is that $\langle m_0 \rangle = 0$, where $\langle (\dots) \rangle$ stands for the average of the quantity (...) over different initial configurations. Now, let us look at the second moment of magnetization. Since the spin-spin correlation $\langle \sigma_i \sigma_j \rangle$ is negligible for $m_0 = 0$, we have that for a fixed t ,

$$\langle M^2 \rangle_{m_0=0} = \frac{1}{L^{2d}} \sum_{i=1}^{L^d} \langle \sigma_i^2 \rangle + \frac{1}{L^{2d}} \sum_i \langle \sigma_i \sigma_j \rangle \approx L^{-d}$$

and by considering the scaling relation (with $b = t^{1/z}$) for the second moment of magnetization, we have according to 1:

$$\begin{aligned} \langle M^2 \rangle_{m_0=0}(t, L) &\approx t^{\frac{-2\beta}{\nu z}} \langle M^2 \rangle_{m_0=0}(1, bL) \\ &= t^{\frac{-2\beta}{\nu z}} (bL)^{-d} \\ &\sim t^{(d-\frac{2\beta}{\nu})/z} \end{aligned} \quad (5)$$

where d is the system dimension.

Using Monte Carlo simulations, many authors have obtained the dynamic exponents θ and z as well as the static ones β and ν , and other specific exponents for several models: Baxter-Wu [35], 2, 3 and 4-state Potts [36, 37], Ising with multispin interactions [38], Ising with competing interactions [39], models with no defined Hamiltonian (celular automata) [40], models with tricritical point [41], Heisenberg [42], protein folding [43] and so on.

The sequence to determine the static exponents from short time dynamics is: first we determine z , performing Monte Carlo simulations that mixes initial conditions [36], and consider the power law for the cumulant

$$F_2(t) = \frac{\langle M^2 \rangle_{m_0=0}}{\langle M \rangle_{m_0=1}^2} \sim t^{d/z}. \quad (6)$$

This ratio has proven to be useful for the calculation of the exponent z for the several spin models governed

by Boltzmann-Gibbs Statistical Mechanics but its application also includes models with spin-flip based on generalized statistics [44]. In this technique, graphs of $\ln F_2$ against $\ln t$ lay on the same straight line for different lattice sizes, without any re-scaling in time, yielding more precise estimates for z . Although it seems clear from Eq. (6), it is worth to stress here that two independent runs are necessary in order to calculate the ratio F_2 : In one of them $m_0 = 0$, while in the other one $m_0 = 1$.

Equations (4), (2), and (6) solve the problem in determining the dynamic critical exponents θ and z . But the ability of short-time Monte Carlo simulations goes beyond the evaluation of dynamic critical exponents, in the sense that this technique also allows us to obtain the static critical exponents which will be discussed in sequence.

Starting from $m_0 = 1$, we have the expected power law described by Eq.(3), so considering $\ln M(t, \tau)$, we must expect

$$\left. \frac{\partial \ln M(t, \tau)}{\partial \tau} \right|_{\tau=0} \sim t^{\frac{1}{\nu z}} \quad (7)$$

which is obtained by differentiating the quantity $\ln M(t, \tau)$ in relation to reduced temperature $\tau = (T - T_c)/T_c$. When dealing with Monte Carlo simulations, the partial derivative is approximated in first order by the difference

$$\left. \frac{\partial \ln M(t, \tau)}{\partial \tau} \right|_{\tau=0} \approx \frac{1}{2\varepsilon} \ln \left[\frac{M(t, T_c + \varepsilon)}{M(t, T_c - \varepsilon)} \right] \quad (8)$$

where $\varepsilon \ll 1$. It is clear from Eq. (8) above that two independent simulations are necessary to obtain the exponent $1/\nu z$: one of them evolves at the temperature $T_c + \varepsilon$, whereas the other one evolves at $T_c - \varepsilon$.

Therefore, with \hat{z} estimated from Eq.(6) we obtain the estimated $\hat{\nu}$ according to $(\widehat{\nu z})^{-1}$ obtained from Eq.(7), by calculating the product:

$$\hat{\nu} = \left[\hat{z} \cdot (\widehat{\nu z})^{-1} \right]^{-1}$$

where the uncertainty in $\hat{\nu}$ is calculated through uncertainty of z (σ_z) and the uncertainty of $(\widehat{\nu z})^{-1}$ ($\sigma_{(\nu z)^{-1}}$), previously obtained by statistics over n_s different seeds, according to the error propagation equation

$$\sigma_\nu = \sqrt{\frac{\sigma_z^2}{\hat{z}^4 (\widehat{\nu z})^{-1}^2} + \frac{\sigma_{(\nu z)^{-1}}^2}{\hat{z}^2 (\widehat{\nu z})^{-1}^4}}$$

Finally, in order to obtain an estimate $\hat{\beta}$, we firstly estimate $(\widehat{\beta/\nu z})$ obtained from the magnetization decay (3) and after we perform the product

$$\hat{\beta} = (\widehat{\beta/\nu z}) \cdot \left[(\widehat{\nu z})^{-1} \right]^{-1}$$

and the propagated error is directly calculated as a function of the respective uncertainties:

$$\sigma_\beta = \sqrt{\frac{\sigma_{(\beta/\nu z)}^2}{(\widehat{\nu z})^{-1}^2} + \frac{(\widehat{\beta/\nu z})^2 \sigma_{(\nu z)^{-1}}^2}{(\widehat{\nu z})^{-1}^4}}$$

Here, it is important to mention that the ratio β/ν already should have been previously calculated by the evaluated $(\widehat{\beta/\nu z})$ from Eq.(3) and \hat{z} from Eq.(6) such that:

$$\widehat{\beta/\nu} = (\widehat{\beta/\nu z}) \cdot \hat{z} \quad (9)$$

Not only quantities related to the moments of the magnetization can explain the non-equilibrium aspects of phase transitions and critical phenomena, but also those related to the first passage time probabilities and variations of this topic (see e.g [45],[46]). By considering this approach and under the same nonequilibrium conditions, a new exponent was initially proposed by [45]: the global persistence exponent θ_g . It is related to the probability $P(t)$ that the global order parameter has not changed sign up to time t after a quench to T_c , according to expected power law behavior

$$P(t) \sim t^{-\theta_g}. \quad (10)$$

As argued by Majumdar *et al.* [45], if the dynamics of the global order parameter is described by a Markovian process, θ_g is not a new independent exponent and it can be related to other critical exponents,

$$\theta_g z = \omega z - d + 1 - \eta/2. \quad (11)$$

where ω is the autocorrelation exponent in the expected power law [47]: $A(t, t' = 0)_{m_0=0} = (1/L^d) \langle \sum_i \sigma_i(t) \sigma_i(0) \rangle \sim t^{-\omega}$, where $\sigma_i(t)$ is the value of the spin variable s_i at the site i of a d-dimensional system of linear size L , assumed, at instant t , z is the dynamic critical exponent defined as $\tau \propto \xi^z$, where τ and ξ are time and spatial correlation lengths, respectively. However, the time evolution of the order parameter is, in general, a non-Markovian process and θ_g turns out to be a new independent critical exponent describing the evolving of the stochastic dynamic process toward the equilibrium.

In order to evaluate the persistence probability $P(t)$, we first define $\rho(t)$ as the fraction of runs for which the magnetization changes its sign for the first time at the instant t . Our probability $P(t)$ is numerically calculated from the cumulative distribution function of such $\rho(t)$. So, $P(t)$ describes the probability of magnetization does not cross the origin up to time t ,

$$P(t) = 1 - \sum_{t'=1}^t \rho(t'). \quad (12)$$

We start our simulations with a random initial condition, where $\langle m_0 \rangle = 0$. Here it is important to mention that

such a concept is very versatile and it has been applied to characterize several applications such as tricritical points [48], besides interdisciplinary applications such as: analysis of bankruptcies of players in public goods games [49], Econophysics [50] and many others. So it can also be interesting, for example, to study Lifshitz points in spin models.

The target of this paper is to enlarge our knowledge of the of the ANNNI model, by studying the ferromagnetic-paramagnetic phase-transition with special attention to the Lifshitz point (LP). The layout of this paper is as follows: In section (II) we give more details about numerical simulations that will be performed at the Lifshitz point. Moreover, we describe a simple method recently developed by R. da Silva et al. in [44] that refines the critical parameters based on the best determination coefficient in linear fit $\ln\langle M \rangle$ versus $\ln t$. In this same section we present a first part of our results, where we explicitly show the refinement of critical temperatures of second order line (ferromagnetic-paramagnetic) up to the Lifshitz point. Finally in section (III) we present our estimates for the critical exponents and in this case we divide our results in two branches: In the branch (A), we evaluate critical exponents (only z and β/ν) for each temperature estimated along critical line previously estimated by the refinement process. In these first calculations, the aim is only the monitoring of the behavior of these two exponents (one dynamic and the other static) to show the pronounced difference between Ising-like points and the Lifshitz point. In the second branch (B) of this same section we present the complete results and studies for both dynamic (θ , θ_g , and z) and static (β and ν) critical exponents specifically for the Lifshitz point, comparing the later with results obtained in previous experimental and theoretical works. Finally, in section (IV) we summarize and briefly discuss the main results of this paper.

II. MONTE CARLO SIMULATIONS

Monte Carlo simulations were performed on simple rectangular lattices with linear dimensions L_x , L_y , and L_z and periodic boundary conditions. The spin states were updated by using the one-spin-flip heat-bath algorithm. For the location of the LP, it was used as basis the result obtained by Henkel and Pleimling [18]: ($-J_2/J_1 = 0.270 \pm 0.004$; $k_B T/J_1 = 3.7475 \pm 0.005$).

For the ANNNI model the order parameter corresponds to time-dependent magnetization, defined as an average over all $L_x \times L_y \times L_z$ spins and over the different N_s runs:

$$\langle M \rangle(t) = \frac{1}{n_s L^3} \sum_{i=1}^{n_s} \sum_{x,y,z} \sigma_{x,y,z}^{(i)}(t) \quad (13)$$

where the index $i = 1, \dots, N_s$ denotes the corresponding run of a simulation. The ordered state is ferromagnetic, with all (or most of) the spins pointing either up or down.

As discussed in the previous section, the lattice's initial condition depends on the scaling relation considered: a) $\langle m_0 \rangle = 0$ – Eq. (4), b) $m_0 = 0$ – Numerator of Eq. (6), c) $m_0 = 1$ Eqs.(3), (8), and d) m_0 fixed, but with random configurations considering a sharp preparation (2).

Here we address time dependent MC simulations in the context of so-called short time dynamics. Before evaluation of some critical exponents and the complete study of the Lifshitz point (next section), also in this section we apply the refinement method to estimate the critical parameters of several points along second order line including the Lifshitz point itself.

The algorithm to estimate the critical temperature is divided in two stages: i) a coarse grained location; ii) fine scale refinement. In stage i), since the magnetization must behave as a power law $\langle M \rangle \sim t^{-\beta/\nu z}$, by fixing a specific α -value, we conjecture that changing $J_1/k_B T_c$ from $J_1/k_B T_c^{(\max)}$ up to $J_1/k_B T_c^{(\min)}$, the corresponding best $J_1/k_B T_c^{(best)}$ is the one that leads to the best linear behavior of $\ln\langle M \rangle$ versus $\ln t$. We have considered $n_s = 400$ realizations, with initial magnetization $m_0 = 1$. For each $\alpha = -J_2/J_1$ changing from 0 up to 0.27, with displacement $\Delta\alpha = 0.03$ between the values, where $J_0 = J_1$ for all of our calculations, we changed $J_1/k_B T_c$ from $J_1/k_B T_c^{(\max)} = 0.26684456\dots$ up to $J_1/k_B T_c^{(\min)} = 0.22165413\dots$. These extreme values were extracted from the literature, since they correspond to best known estimates for the 3D Ising model ($\alpha = 0$ which corresponds to $k_B T_c/J = 4.5115333351\dots$) and LP ($\alpha = 0.27$ which corresponds to $k_B T_c/J = 3.7475\dots$) respectively. Just as a safeguard, we enlarge this interval, by performing $J_1/k_B T_c^{(\max,0)} = 0.28$ and $J_1/k_B T_c^{(\min,0)} = 0.21$.

So, for each input α -value, by using $\Delta^{(0)}(J_1/k_B T_c) = 0.002$, we span our temperatures on a range described by parametrization $J_1/k_B T_c = J_1/k_B T_c^{(\min)} + j \Delta^{(0)}(J_1/k_B T_c)$, $j = 0, \dots, 32$, so for each temperature, a linear fit is performed and one calculates the determination coefficient of the fit as:

$$r = \frac{\sum_{t=1}^{N_{MC}} (\overline{\ln\langle M \rangle} - a - b \ln t)^2}{\sum_{t=1}^{N_{MC}} (\overline{\ln\langle M \rangle} - \ln\langle M \rangle(t))^2} \quad (14)$$

with $\overline{\ln\langle M \rangle} = (1/N_{MC}) \sum_{t=1}^{N_{MC}} \ln\langle M \rangle(t)$, where N_{MC} is the number of Monte Carlo sweeps. In our experiments, we have used $N_{MC} = 150$ MC steps, discarding the initial 30 MCsteps for more robust estimates. Hence, $r = 1$ means an exact fit, and so the closer r is from the unity, the better is the fit. Here, a and b are the linear coefficient and the slope in the linear fit $\ln\langle M \rangle$ versus $\ln t$, respectively. From b , one estimates the exponent $\beta\nu/z$.

After, one finishes this part of our refinement method (i), we pass to the second part of refinement, the fine scale stage (ii). Starting from the critical temperature $k_B T_c^{(1)}(q)/J_1$ obtained in the first stage, we use the process considering a more refined displace-

ment, i.e., $\Delta^{(1)}(J_1/k_B T_c) = 1 \cdot 10^{-4}$. So, by using $J_1/k_B T_c^{(\min,1)} = J_1/k_B T_c^{(1)} - \Delta^{(0)}(J_1/k_B T_c)$ and $J_1/k_B T_c^{(\max,1)} = J_1/k_B T_c^{(1)} + \Delta^{(0)}(J_1/k_B T_c)$, we consider a new parametrization $J_1/k_B T_c = J_1/k_B T_c^{(\min,1)} + \Delta^{(1)}(J_1/k_B T_c)j$, with $j = 0, \dots, 41$. Hence, we determine a new best temperature $k_B T_c^{(2)}/J_1$ corresponding to the maximum value of r .

Plot 2 shows the determination coefficient (r) as function of temperature for two extremal cases $\alpha = 0.03$ and $\alpha = 0.27$.

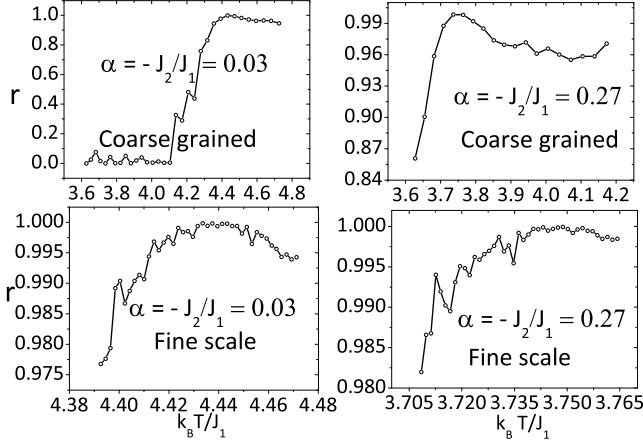


FIG. 2. Determination coefficient (r) as function of temperature for two cases $\alpha = 0.03$ and $\alpha = 0.27$. The upper plots correspond to coarse grained regime (i) of process ($\Delta(J_1/k_B T) = 2.10^{-3}$) while the lower plots correspond to fine scale regime (ii) of process ($\Delta(J_1/k_B T) = 1.10^{-4}$).

The upper plots correspond to the coarse grained regime (first refinement – i) of process ($\Delta(J_1/k_B T) = 2.10^{-3}$) while the lower plots correspond to the fine scale regime (second refinement – ii) ($\Delta(J_1/k_B T) = 1.10^{-4}$). The estimated temperatures after two refinement states for all studied α -values can be observed in table I.

Since our final refinement has a precision of $\Delta(J_1/k_B T_c) = \Delta(\beta_c) = 10^{-4}$, which means $\Delta(T_c) = \Delta(\beta_c)T_c^2/(1 + \Delta(\beta_c)T_c)$, we have a precision with 3 digits for temperature. Therefore, we show our results for critical temperatures with 3 significant elements (second column in table I). It is important to mention that our estimates corroborate literature results: For example, for $\alpha = 0$ we have as 3D Ising estimate $k_B T_c/J_1 = 4.513$ which yields an excellent agreement with estimates via equilibrium Monte Carlo simulations [51]. For $\alpha = 0.27$, we have $k_B T_c/J_1 = 3.748$ as best estimate for the LP's critical temperature, which also agrees with the estimate obtained by Henkel and Pleimling [18] $k_B T/J_1 = 3.7475 \pm 0.0050$.

Here, it is important to mention that in order to check the robustness of our method, we performed the same refinement process inverting the input, i.e., we fixed $k_B T/J_1 = 3.7475$ and we refine the value α . For the

$\alpha = -J_2/J_1$	$k_B T_c/J_1$	r
0.00	4.513	0.99993
0.03	4.434	0.99982
0.06	4.364	0.99990
0.09	4.289	0.99990
0.12	4.213	0.99993
0.15	4.126	0.99991
0.18	4.039	0.99988
0.21	3.956	0.99991
0.24	3.852	0.99989
0.27	3.748	0.99992

TABLE I. Critical values obtained by refinement procedure after two stages (coarse-grained and fine scale). Here, the values obtained for $\alpha = 0$ and $\alpha = 0.27$ correspond to our estimates of the critical temperatures of 3D-Ising model and Lifshitz point respectively.

sake of simplicity, here we perform only one refinement in a shorter interval spanning α -values from 0.26 to 0.28 with $\Delta\alpha = 0.001$ which can be observed in Fig. 3.

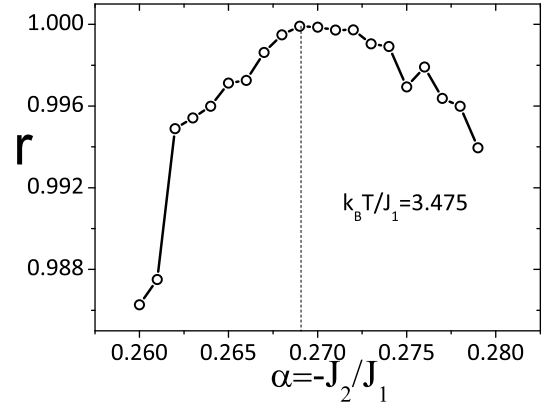


FIG. 3. **Inverted refinement process:** determination coefficient (r) as function of α , which changes from 0.26 up to 0.28 by fixing $k_B T/J_1 = 3.475$. Only one refinement process with $\Delta\alpha = 0.001$ was used. We obtain as best estimate $\alpha = 0.269$, which shows that the method works in both ways.

We find $\alpha = 0.269$ as the best estimate which corroborates the expected value for $k_B T/J_1 = 3.7475$: $\alpha = 0.270(4)$.

So, once we have shown that our time-dependent simulations are calibrated and they corroborate the critical parameters of the main estimates of literature, in the next section, our focus is to calculate the critical exponents via time-dependent Monte Carlo simulations of LP. First, we present some exponents (z and β/ν) to monitor their behavior along the second order transition. After, we show a detailed study for the Lifshitz point, by calculating all (static and dynamic) critical exponents obtaining

	$80 \times 80 \times 80$	$80 \times 80 \times 10$	$120 \times 120 \times 10$
$\beta/\nu z$, Eq.(3)	400	3200	1400
$(d - \frac{2\beta}{\nu})/z$, Eq.(5)	4000	$3.2 \cdot 10^4$	$1.4 \cdot 10^4$
$1/\nu z$, Eq.(7)	2000	$1.6 \cdot 10^4$	7000
θ , Eq.(2)	14000	14000	14000
θ , Eq.(4)	28000	28000	28000
θ_g , Eq.(10)	14000	14000	14000

TABLE II. Number of runs used in simulations for different size lattices

error bars by performing repetitions of simulations under different seeds. We also studied some differences between rectangular and cubic lattices.

III. RESULTS

In this work we perform short-time Monte Carlo simulations in simple rectangular lattices of size $L_x \times L_y \times L_z$ and not only for $L_x = L_y = L_z = L$. Thus, at each instant t of the simulation, the value of any measured quantity is given by its average over n_s runs according to equation (13), which denotes an average over different repetitions (trajectories with different sequences of pseudo-random numbers).

In order to obtain error bars in our simulations for the LP, we used $n_b = 5$ sets of n_s runs corresponding to different seeds for the random numbers generator. For our calculations, we first used cubic lattices ($80 \times 80 \times 80$) to evaluate only two exponents (z and β/ν) along the second order line by performing MC simulations using as input the critical parameters obtained in the previous section. We monitor the behavior of these two exponents directly obtained as a function of $k_B T_c/J_1$.

Second, for the Lifshitz point we used three different lattices $80 \times 80 \times 80$, $80 \times 80 \times 10$, and $120 \times 120 \times 10$ in order to study the possible distortions under rectangular regions. For each lattice size, the number of runs used in the simulations in order to obtain the exponents given in Eqs. (3), (5), (7), (4), (2), and (10) are shown in table II.

Due to the axial anisotropy present in the ANNNI model, the critical behavior in the neighborhood of the LP is governed by two correlation lengths, ξ_z and ξ_{xy} with different critical exponents ($\nu_z = \frac{1}{2}\nu_{xy}$) [14]. Therefore, at the LP, in the case of the simple cubic lattice, the resulting critical exponent ν may be either the exponent $\nu_z(\nu_{xy})$ or a combination of these exponents. Therefore, in order to calculate the static critical exponent ν for the Lifshitz point, we also considered not only cubic lattices in our study but also rectangular lattices.

$\alpha = -J_2/J_1$	z	β/ν
0.00	2.068	0.5118
0.03	2.069	0.4465
0.06	2.061	0.4807
0.09	2.076	0.4777
0.12	2.086	0.4746
0.15	2.137	0.4478
0.18	2.172	0.4334
0.21	2.197	0.4676
0.24	2.290	0.4082
0.27	2.338	0.3867

TABLE III. Monitoring of critical exponent z and the ratio of exponents β/ν along the second order line previously estimated by time-dependent MC simulations

A. Monitoring the critical exponents of the ANNNI model

Using as input the critical parameters previously estimated in section (II), we have calculated the exponent z from the time-dependence of the ratio F_2 (Eq.(6)) for cubic lattices with $L = 80$. Since z was calculated, the time evolving from ordered state (Eq. 3) which was used to compose F_2 is taken also to obtain an estimate of $(\beta/\nu z)$ and since we have an estimate of z by equation Eq.(9) we obtain an estimate of β/ν .

Performing MC simulations up to 150 MCsteps and discarding the initial 30 MCsteps for more robust estimates we estimate these exponents for all α -values corresponding to the critical temperatures which were previously obtained in section (II), considering the limits: 3D-Ising like ($\alpha = 0$) up to the Lifshitz point ($\alpha = 0.27$). We set our simulations exactly at the temperatures obtained by our refinement procedure. The time evolving of the magnetization $\langle M(t) \rangle_{m_0=1}$, of its second moment $\langle M^2(t) \rangle_{m_0=0}$ and of $F_2(t)$ can be observed in figure 4.

The estimates of z and β/ν are summarized in table III. We can observe that z is universal when J_2 is small, i.e., the interaction among second neighbors in z direction is not pronounced and $z \approx 2.06$ which is expected for universality class of the 3D Ising model.

However, in the neighborhood of the Lifshitz point, the exponent z has a sensitive increasing in relation to Ising like behavior. The ratio of exponents β/ν changes in an interval $[0.38, 0.52]$ but not monotonically as occurs with z . In the next subsection we will study all details of the Lifshitz point, taking into consideration error bars obtained by considering simulations with different seeds, since we observed a notorious difference between this point ($\alpha = 0.27$) and the authentic 3D Ising model ($\alpha = 0.0$).

B. Lifshitz Point

In this subsection, we finally present a detailed study of critical exponents of the Lifshitz point. Initially we considered cubic lattices $L_x = L_y = L_z = 80$. Here it is important to stress that we used $\alpha = 0.27$ and $k_B T_c / J_1 = 3.7475$ (estimate obtained by Henkel and Pleimling [18]) to perform the simulations.

So, first of all, from Monte Carlo simulations we obtained the exponents for the Lifshitz point defined by equations (6) (that uses the equations (3) and (5)), (7), (2), and (4). The log-log curves for the Lifshitz point for these quantities considering the error bars obtained by 5 different seeds are shown in Fig.(5). For equation (2) we show (for the sake of simplicity) only the evolution for $m_0 = 0.04$.

We have obtained the critical exponents $\beta = 0.226(2)$, $\nu = 0.60(1)$, $z = 2.34(2)$, $\theta = 0.17(2)$ (from Eq. 4) and $\theta = 0.163(3)$ (Eq. 2). For this last case the results were obtained by performing simulations with 3 different initial magnetizations $m_0 = 0.02$, $m_0 = 0.04$ and, $m_0 = 0.08$. By obtaining the exponent for each value with error bars obtained by 5 seeds, we considered a linear fit to obtain an extrapolation $m_0 \rightarrow 0$, which corresponds to linear coefficient in the fit θ versus m_0 .

To verify whether the ferromagnetic ordering is affected by increasing the linear dimension L_z , we perform extra MC simulations for the temporal evolution of magnetization from ordered initial state $m_0 = 1$, considering the following rectangular lattices: $20 \times 20 \times 200$, $20 \times 20 \times 700$, and $20 \times 20 \times 1000$. Here we are only interested in the qualitative plots of $\langle M(t) \rangle$ versus t . We used in all cases just $n_s = 400$ runs. In Fig. 6 we find identical log-log plots for different rectangular lattices analyzed, which corroborates that ferromagnetic ordering does not depend on linear dimension L_z , despite the increasing of the total number of spins on the lattice.

Since the order parameter is the magnetization and the xy interactions are ferromagnetic, the ordering occurs mainly due to these interactions. On the other hand, there are competing interactions along the z axis, which cannot sustain the ferromagnetic ordering of the system. This fact is illustrated in Fig. 7, where the magnetizations $\langle M(t) \rangle$ obtained from simulations for lattices $50 \times 50 \times 10$ and $50 \times 10 \times 50$ are shown. In Fig 7 we clearly see that the order parameter decays faster for the lattice with a smaller xy plane ($50 \times 10 \times 50$).

Therefore, we conclude that the best results will be obtained from lattices with bigger xy planes, irrespective of the value L_z . However, we must stress here, these conclusions are valid in the short-time regime. On the other hand, via equilibrium MC simulations, which were performed in a simple cubic lattice ($24 \times 24 \times 24$), Kaski and Selke [17] obtained the critical exponent $\nu = 0.51(4)$ corresponding to a combination of the exponent ν_z and ν_{xy} due to anisotropy present in the LP. In order to obtain the critical exponent $\nu_z = 0.33(3)$ shown in table IV that show exponents for our comparison extracted from

	1st order ε [14]	2nd order ε [54]	Monte Carlo	MnP [55]
β	1/4	0.220	0.19(2) [17] 0.238(5) [18]	
ν_z	5/16	0.348	0.33(3)	0.30(2)
ν_{xy}	5/8	0.696	0.66 [17]	0.60(4)

TABLE IV. Static critical exponents β , ν_z , and $\nu_{xy}=2\nu_z$ at the LP extracted from literature.

	$80 \times 80 \times 80$	$80 \times 80 \times 10$	$120 \times 120 \times 10$
β	0.226(2)	0.227(1)	0.229(2)
z	2.34(2)	2.296(2)	2.30(1)
ν_{xy}	0.60(1)	0.615(3)	0.618(4)
θ	0.17(2) Eq. (4) 0.163(3) Eq. (2)	0.16(2) Eq. (4) 0.180(6) Eq. (2)	0.16(2) Eq. (4) 0.184(1) Eq. (2)
θ_g	0.336(4)	0.330(5)	0.336(6)

TABLE V. Static and dynamic critical exponents β , z , ν_{xy} , θ , and θ_g obtained in the present work for different lattice sizes.

literature obtained for different methods, these authors divided the lattice into sub-cells $24 \times 24 \times L$. By using this procedure, Kaski and Selke [17] were able to capture the spacial correlations ξ_z and from the slope of Binder's cumulant [52, 53], they estimated the value of ν_z which is also shown in table IV.

In the following we show the results obtained in this work for the lattice sizes $80 \times 80 \times 10$ and $120 \times 120 \times 10$. We estimated the critical exponents $\beta = 0.227(1)$, $z = 2.296(3)$ and $\nu = 0.615(3)$ ($80 \times 80 \times 10$) and $\beta = 0.229(2)$, $z = 2.30(1)$ and $\nu = 0.618(4)$ ($120 \times 120 \times 10$).

Finally, we also study the global persistence for the Lifshitz point. For a simple comparison, we also performed simulations for $\alpha = 0$ (that corresponds to the three-dimensional Ising model). The same procedure used in the previous simulations (5 seeds to obtain error bars) was replicated here as well. The figure 8 shows the different time evolutions of global persistence $P(t)$ for the two different points.

We obtain for lattices $80 \times 80 \times 80$, $\theta_g = 0.336(4)$ for the Lifshitz point. This value is smaller than $\theta_g = 0.384(6)$ found for the 3D Ising model. This value for the Lifshitz point seems to be corroborated for rectangular lattices (compatible with error bars) where we observed only small changes for rectangular lattices $80 \times 80 \times 10$ and $120 \times 120 \times 10$ (see last row in table V).

Table V summarizes the results of the static and dynamic critical exponents obtained in this work. These results are in very good agreement with the critical exponents obtained in previous works, shown in table IV.

IV. SUMMARY AND DISCUSSION

In this work we estimated the dynamic critical exponents (θ , θ_g , and z) at the Lifshitz point of the ANNNI model, by means of time dependent Monte Carlo simulations. To our knowledge, this is the first attempt in order to obtain such exponents.

We have also obtained the static and critical exponents β and ν by exploiting scaling relations, valid in the short-time regime (out of equilibrium), involving the order parameter and its second moment. Our estimates (see table V) are in very good agreement with previous experimental and theoretical works (see table IV)

Moreover we applied a refinement procedure to estimate several parameters for the critical points along second order transition line from the 3D Ising point ($-J_2/J_1 = 0$) up to Lifshitz point ($-J_2/J_1 = 0.27$) and we follow the behavior of some exponents along this line. We can observe that z is universal when J_2 is small, i.e., the interaction among second neighbors in z direction is

not pronounced resulting in $z \approx 2.06$ which is exactly expected for universality class of 3D Ising. However, in the neighborhood of the Lifshitz point, the exponent z has a sensitive increase resulting in $z \approx 2.34$. Finally, we also observe power law behavior for the global persistence ($P(t)$, probability that the sign of the magnetization does not change until the time t starting from random configurations with small magnetization). We find $\theta_g = 0.336(4)$ ($\alpha = 0.27$) for the LP that is smaller than 3D-Ising estimate ($\alpha = 0$) $\theta_g = 0.384(6)$.

ACKNOWLEDGEMENTS

The authors are partly supported by the Brazilian Research Council CNPq. Authors also thank CESUP (Super Computer Center of Federal University of Rio Grande do Sul) as well as Prof. Leonardo G. Brunet (IF-UFRGS) for the available computational resources and support of Clustered Computing (ada.if.ufrgs.br) and Prof. Mendeli H. Vainstein (IF-UFRGS) for carefully reading our manuscript.

-
- [1] P. Bak, Rep. Prog. Phys. 45, 587-629(1982).
 - [2] G. Toulouse, Commun. Phys. 2(4), 115-119(1977) .
 - [3] B. R. Cooper, Solid State Phys. 21, 393(1968)
 - [4] M.A.Ruderman, C. Kittel , Phys. Rev. 96, 99-102(1954)
 - [5] T. Kasuya, Prog. Theor. Phys. 16, 45-57(1956) .
 - [6] K.Yosida, Phys. Rev. 106, 893-898(1957)
 - [7] R. J. Elliott, Phys. Rev. 124, 346-353(1961) .
 - [8] M. E. Fisher, W. Selke, Phys. Rev. Lett. 44, 1502-1505(1980).
 - [9] W. Selke, Phys. Rep. 170, 213-264(1988).
 - [10] J. M. Yeomans, in Solid State Physics, edited by H. Ehrenreich and D. Turnbull (Academic Press, San Diego (CA), 1988), Vol. 41, pp. 151-200.
 - [11] W. Selke, in Phase Transitions and Critical Phenomena, edited by C. Domb and J. L. Lebowitz (Academic Press, London, 1992), Vol. 15, pp. 1-72.
 - [12] P. Bak, J.von Boehm, Phys. Rev. B 21, 5297-5308(1980).
 - [13] T. Garel, P. Pfeuty, J. Phys. C 9 L245-L249(1976).
 - [14] R. M. Hornreich, M. Luban, S. Shtrikman, Phys. Rev. Lett. 35 (25), 1678-1681(1975).
 - [15] S. Redner, H. E. Stanley, Phys. Rev. B 16 (11) 4901-4906(1977).
 - [16] W. Selke, Z. Phys. B 29 133-137(1978).
 - [17] K. Kaski, W.Selke, Phys. Rev. B 31(5) 3128-3130(1985).
 - [18] M. Henkel, M. Pleimling, Comput. Phys. Commun. 147, 419-422(2002).
 - [19] U. Wolf, Phys. Rev. Lett. 62(4), 361-364(1989).
 - [20] R. M. Hornreich, J. Magn. Mater.15(18), 387(1980).
 - [21] Z. Mo, M. Ferer, Phys. Rev. B 43 (13) 10890-10905(1991).
 - [22] C. C. Becerra, Y. Shapira, N. F. de Oliveira Jr., T. S. Chang, Phys. Rev. Lett. 44, 1692(1980).
 - [23] Y. Shapira, C. C. Becerra, N. F. de Oliveira Jr, T. S. Chang, Phys. Rev. B 24(5) 2780-2806(1981).
 - [24] V. Bindilatti, C. C. Becerra, N. F. de Oliveira Jr., Phys. Rev. B 40 9412(1989).
 - [25] Z. B. Li, L. Schülke, and B. Zheng, Phys. Rev. E 53, 2940 (1996)
 - [26] R. Folk, W. Selke, Phys. Lett. A 69, 255 (1978)
 - [27] A. Basu, J K Bhattacharjee, J. Phys. A37, 1111(2004)
 - [28] T. Ala-Nissila, J. D. Gunton, K. Kaski, Phys. Rev. B 37 (1), 179-195(1988)
 - [29] M. Cheon, I. Chang, Phys. Rev. Lett. 86, 4576-4579 (2001)
 - [30] H. K. Janssen, B. Schaub, B. Shmittmann, Z. Phys. B 73(4), 539-549(1989).
 - [31] D. A. Huse, Phys. Rev. B 40, 304(1989).
 - [32] B. Zheng, Int. J. Mod. Phys. B12, 1419-1484(1998).
 - [33] E. V. Albano, M. A. Bab, G. Baglietto, R. A. Borzi, T. S. Grigera, E. S. Loscar, D. E. Rodriguez, M. L. Rubio Puzzo, and G. P. Saracco, Rep. Prog. Phys. 74, 026501 (2011)
 - [34] T. Tome, M. J. de Oliveira, Phys. Rev. E 58(4), 4242-4245(1998).
 - [35] E. Arashiro and J. R. Drugowich de Felício, Phys. Rev. E **67**, 046123 (2003)
 - [36] R. da Silva, N. A. Alves, J. R. Drugowich de Felício, Phys. Lett. A 298, 325-329(2002).
 - [37] R. da Silva and J. R. Drugowich de Felício, Phys. Lett. A 333, 277 (2004); H.A. Fernandes, E. Arashiro, J.R. Drugowich de Felício, A.A. Caparica Physica A 366, 255-264 (2006); E. Arashiro, H.A. Fernandes, J.R. Drugowich de Felício, Physica A 388, 4379-4386 (2009)
 - [38] C. S. Simões, J. R. Drugowich de Felício, Mod. Phys. Lett. B 15(15), 487-496(2001).
 - [39] N. Alves Jr., J. R. Drugowich de Felício, Mod. Phys. Lett. B 17(56), 209-218(2003).
 - [40] R. da Silva and N. Alves Jr., Phys. A 350, 263 (2005); T. Tome, J. R. Drugowich de Felício Mod. Phys. Lett. B12

- (21), 873-879(1998).
- [41] R. da Silva, N. A. Alves, J. R. Drugowich de Felício, Phys. Rev. E 66(2), 026130(2002).
 - [42] H. A. Fernandes, R. da Silva, J. R. Drugowich de Felicio, J. Stat. Mech., P10002 (2006).
 - [43] E. Arashiro, J. R. Drugowich de Felício, U. H. E. Hansmann, Phys. Rev. E, 73(4), 40902 (2006); JCP 126, 045107(2007)
 - [44] R. da Silva, J. R. Drugowich de Felício, A. S. Martinez, Phys. Rev. E 85, 066707(2012)
 - [45] S.N. Majumdar, A.J. Bray, S.J. Cornell and C. Sire, Phys. Rev. Lett. **77**, 3704 (1996).
 - [46] S.N. Majumdar and C. Sire, Phys. Rev. Lett. **77**, 1420 (1996)
 - [47] H. K. Janssen, From phase transition to chaos, in: G. Gyoorgyi, I. Kondor, L.Sasvlari, T.Tel (Eds.),Topics in Modern Statistical Physics,WorldScientif, Singapore,1992.
 - [48] R. da Silva, N. A. Alves, J. R. Drugowich de Felício, Phys. Rev. E **67**, 057102 (2003)
 - [49] R. da Silva, Ana L. C. Bazzan, A. T. Baraviera, Sílvia R. Dahmen, Physica A **371**, 610-626(2006)
 - [50] R. da Silva, M. Zembrzusi, F. Correa, L. da C. Lamb, Physica A **389**, 5460-5467(2010)
 - [51] W. Janke and R. Villanova, Nucl. Phys. B 489, 679 (1997).
 - [52] K. Binder, Phys. Rev. Lett. 47(9), 693-696(1981).
 - [53] K.Binder, Z. Phys. B 43(2), 119-140(1981).
 - [54] M. Shpot, H. W. Diehl, Nucl. Phys. B 612(3), 340-372(2001).
 - [55] Y. Shapira, Nato advanced study institutes, in: R. Pynn, A.Skjeltorp(Eds.), Multicritical Phenomena,Vol.106 of B, Plenum, New York, pp.53-71(1984).

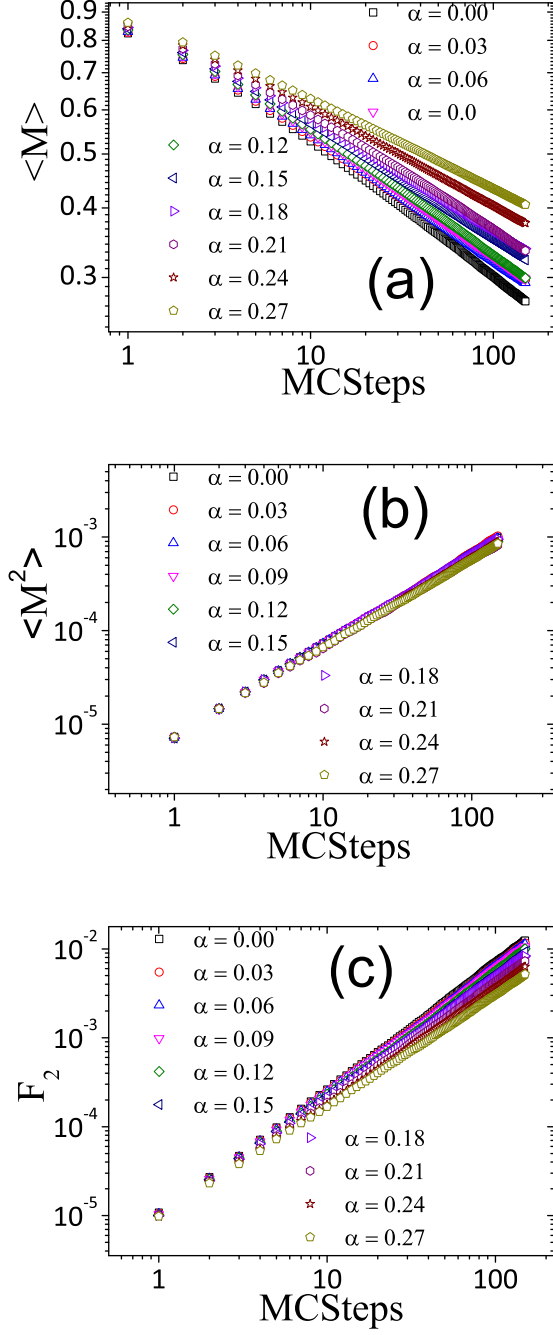


FIG. 4. (Color Online) Time evolving of $\langle M(t) \rangle_{m_0=1}$ (plot a), $\langle M^2(t) \rangle_{m_0=0}$ (plot b), and $F_2(t)$ (plot c) for all critical temperatures previously estimated (corresponding to the different α -values)

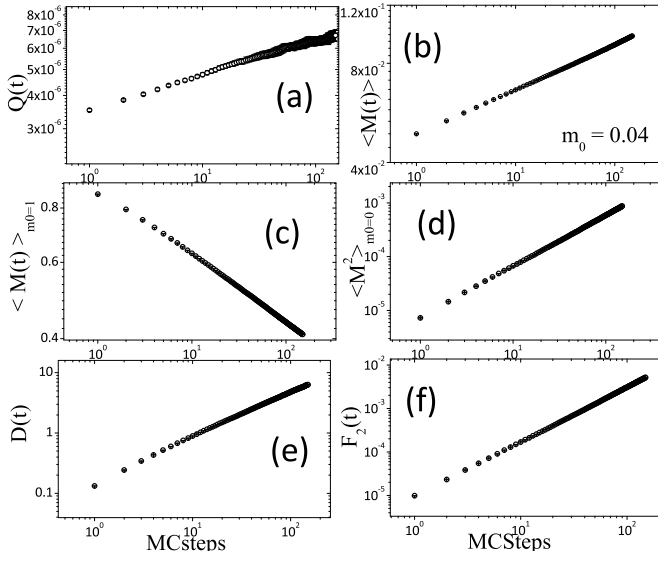


FIG. 5. (a) log-log curve of $Q(t)$ against t , for the lattice size $80 \times 80 \times 80$ for the Lifshitz point by using $\alpha = 0.27$ and $k_B T_c / J_1 = 3.7475$. The plots (b), (c), (d), (e) and (f) correspond to same plots plot for $\langle M(t) \rangle_{m_0=0.04}$, $\langle M(t) \rangle_{m_0=1}$, $\langle M^2(t) \rangle_{m_0=0}$, $D(t)$, and $F_2(t)$.

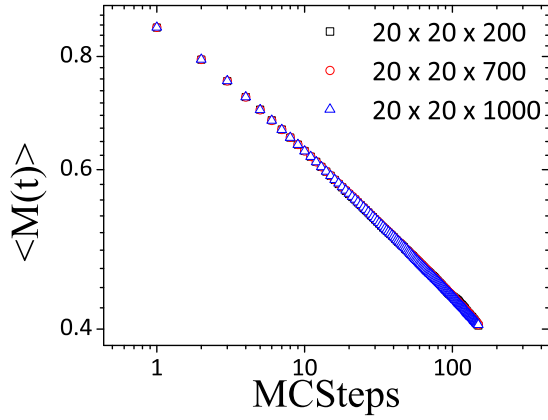


FIG. 6. (Color Online) Log-log curves of $\langle M(t) \rangle$ against t obtained from the simulations performed for the lattice sizes $20 \times 20 \times L_z$, where $L_z > 20$ and $m_0 = 1$ (ordered initial state).

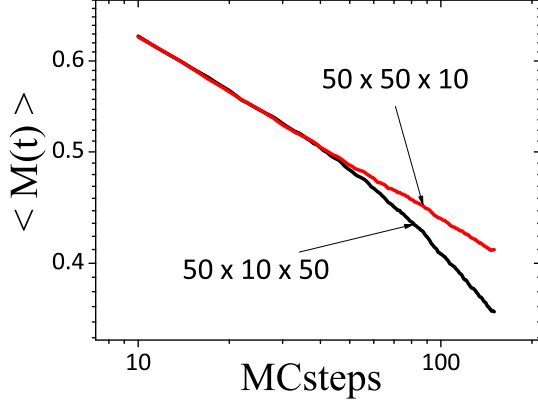


FIG. 7. (Color online) Log-log curves of $\langle M(t) \rangle$ against t obtained from the simulations performed for the lattice sizes $50 \times 50 \times 10$ and $50 \times 10 \times 50$, starting from the initial condition $m_0 = 1$ (ordered initial state). The order parameter decays faster for the lattice with smaller xy planes.

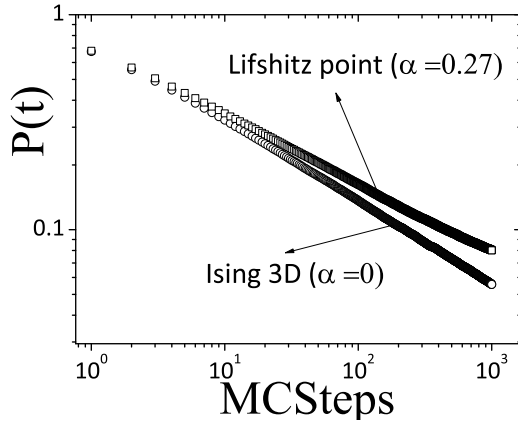


FIG. 8. Time evolving of global persistence for $\alpha = 0$ (**3D Ising model**) $k_B T/J_1 = 4.513$ and $\alpha = 0.27$ (**Lifshitz point**) $k_B T/J_1 = 3.7475$.